Half-Cell Cumulative Efficiency Forecasts Full-Cell Capacity Retention in Lithium-Ion Batteries

Maxwell C. Schulze and Nathan R. Neale*
Chemistry and Nanoscience Center, National Renewable Energy Laboratory, 15013 Denver West Parkway, Golden, Colorado 80401, United States

Synthesis of Si NPs via nonthermal plasma-enhanced chemical vapor deposition

Si NPs were synthesized using a custom-built capacitively coupled plasma reactor with a secondary gas injection system downstream of the primary electrode.[1–3] Briefly, Si NPs with a mean diameter ~30 nm were produced in a quartz tube (19 mm ID, 25 mm OD) as follows. The primary gas feed comprised 10 sccm SiH_4, 80 sccm Ar, and 90 sccm He. 200 sccm SiH_4 were introduced via the secondary gas inlet and the reactor pressure was maintained at 13 Torr for the NP synthesis. A copper ring working electrode was located 25 mm above the secondary gas injection apparatus that served as the ground electrode. An Advanced Energy Cesar 136 generator applied 250 W of forward power at 13.6 MHz. An Advanced Energy VM1000 matching network was used to keep the reflected power at 0–1 W and an estimated ~4 W/cm^3 of delivered power by monitoring the plasma circuit using an Advanced Energy Z'Scan device installed at the working electrode. The produced nanoparticles ($Si@SiH_x$) were collected on a 400-mesh stainless steel filter and transferred into an Ar-filled glovebox with no exposure to air for NP harvesting.

Coating of Si NPs with molecular precursors

N-methyl pyrrolidone was distilled from sodium under nitrogen and toluene was dried using an MBraun commercial solvent purification system. After purification, all solvents were stored and used in an Ar-filled glovebox at with <1 ppm O_2 and H_2O. Si NP coating reactions were performed in in sealed glass vials in an Ar-atmosphere glovebox as follows. A 20 mL glass scintillation vial was charged with 80–100 mg of $Si@SiH_x$ powder, an equivalent mass of a coating precursor molecule (all precursors shown in Scheme 1 in main text), and 2 mL of toluene. For the reaction with vinyl-naphthalene, ~5 mg of radical initiator ABCN was also added to promote reaction of the vinyl group with the $–SiH_x$ NP surface. Each vial was capped and heated at 90˚C for at least 24 hours. Each mixture was cooled, transferred to a 50 mL centrifuge tube with an addition 5 mL toluene, vortexed, and centrifuged 12,500×*g* for 5 minutes to separate the coated Si@R NPs. The supernatant was separated, and the Si@R NPs were washed twice more via the same procedure. Finally, residual solvent was removed by drying the Si@R NPs under vacuum.

Electrode slurry formulation and printing

The electrode slurries were prepared in an Ar-filled glovebox and cast using conventional composite electrode fabrication techniques. Each Si@R NP sample was mixed with a 20 mg/mL polyacrylic acid (PAA, 450 Mw) solution in NMP and Timcal C65 conductive carbon such that the ratio of solids equaled 40:40:20 of Si@R:C65:PAA. The mixtures were stirred at least 1 hour mixing for 90 seconds using a planetary mixer (Mazerustar KK-250S). A Zehntner ZAA 2300 Automatic Film Applicator was used to cast each slurry onto a Cu foil with a wet gap of 250 µm

and casting speed of ~1 cm/s. Each electrode was then dried at 150 ˚C for 4 h in a heated antechamber under vacuum (no exposure to air).

Half-cell assembly and electrochemical cycling

Each Si@R electrode was tested in triplicate in Li-ion half-cells with "GenF" electrolyte (1.08 M $LiPF_6$ in fluoro-ethylene-carbonate:ethylene-carbonate:ethyl-methyl-carbonate 1:2.7:6.3 by weight). Each half-cell was assembled with the following stack order: Positive cell cap, 14 mm diameter punch of a Si@R electrode, 20 µL electrolyte, 19 mm diameter punch of Celgard 2325 separator, coin cell gasket, 20 µL electrolyte, 9/16" diameter punch of Li foil (Alfa Aesar 10769, 0.75 mm thick, 99.9% metals basis, surface cleaned with toothbrush), 1 mm thick stainless-steel (SS) spacer, wave spring, negative cell case. The cells were sealed using a Hohsen automatic hydraulic crimper and allowed to rest for 4 hours at open circuit potential before cycling using the following protocol: Cells were cycled 3 times at a C/20 rate (calculated using mass of electrode punch and specific capacity of Si NPs of 3500 mAh/g) between 0.01–1.5 V vs. Li/Li$^+$, followed by cycling with the same voltage cutoffs at a calculated rate of C/5.
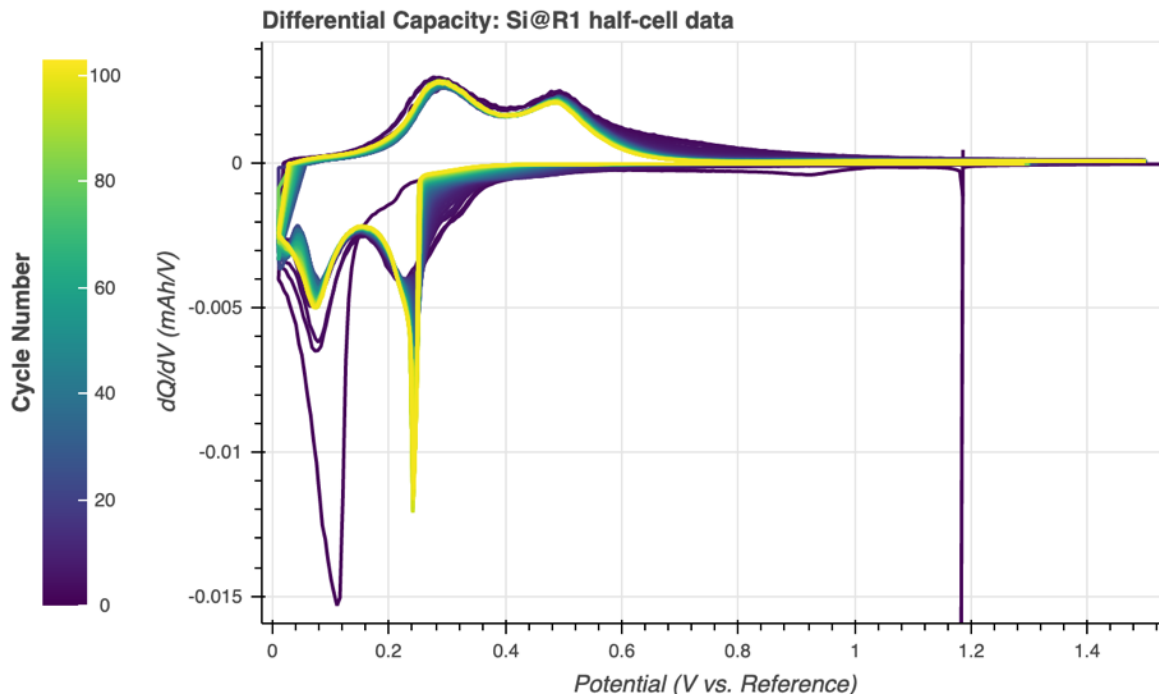

Figure S1. Differential capacity of a half-cell with an electrode made with Si NPs coated with 4-phenyl phenol (Si@R$_1$). The 1st cycle exhibits a single lithiation peak around ~0.1 V vs. Li/Li$^+$ and two delithiation peaks around ~0.3 and ~0.5 V vs. Li/Li$^+$. All subsequent cycles exhibit two lithiation peaks around ~0.25 and ~0.8 V vs. Li and the same two delithiation peaks as the first cycle. The diminishing lower voltage delithiation peak height between cycle 1 through 4 indicates significant lithation charge going towards initial SEI layer formation. The slight shifting of the shoulders of the higher voltage lithiation and delithiation peaks indicate that the SEI evolves some with cycling. The stable height and voltage of the lithiation and delithation peaks following these initial cycles indicates that there is minimal active material loss or impedance rise over the 100 cycles shown.

Considerations for precisely measuring diminishingly small coulombic inefficiency values

As the measured coulombic inefficiency values become <0.1% (CE values >99.9%), it is important to verify that the instrument used to make the measurements can resolve the current, voltage, and time step values finely enough to precisely determine the capacity of each charge and discharge. In fact, specially designed high precision coulometry instruments are often needed to accurately determine CE values that would result in cycle lifetimes more than 1000 cycles.[4–6]
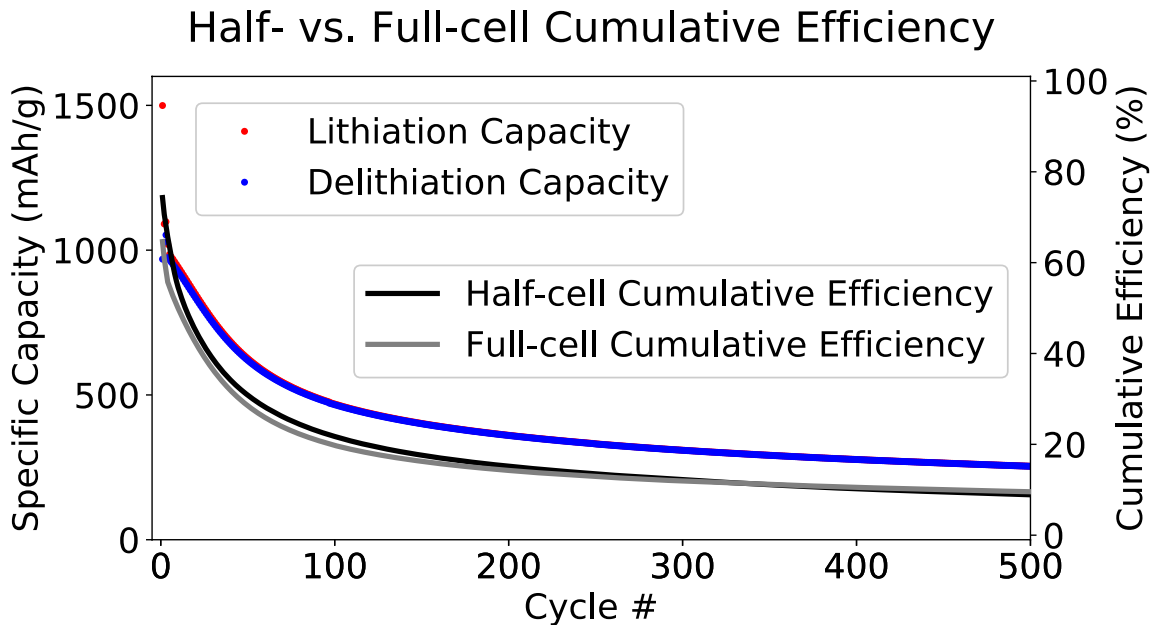

Figure S2. Cycling data of the Si@R$_1$ electrode in a capacity-matched LFP full-cell (red and blue traces) and cumulative efficiency calculated from full-cell CE (grey trace) and half-cell CE data (black trace) from Figure 3. The close tracking of the half-cell cumulative efficiency data to the trajectory of the full-cell reversible capacity data demonstrates that this metric can be used as a semi-quantitative measure of the expected full-cell capacity retention using solely half-cell data.
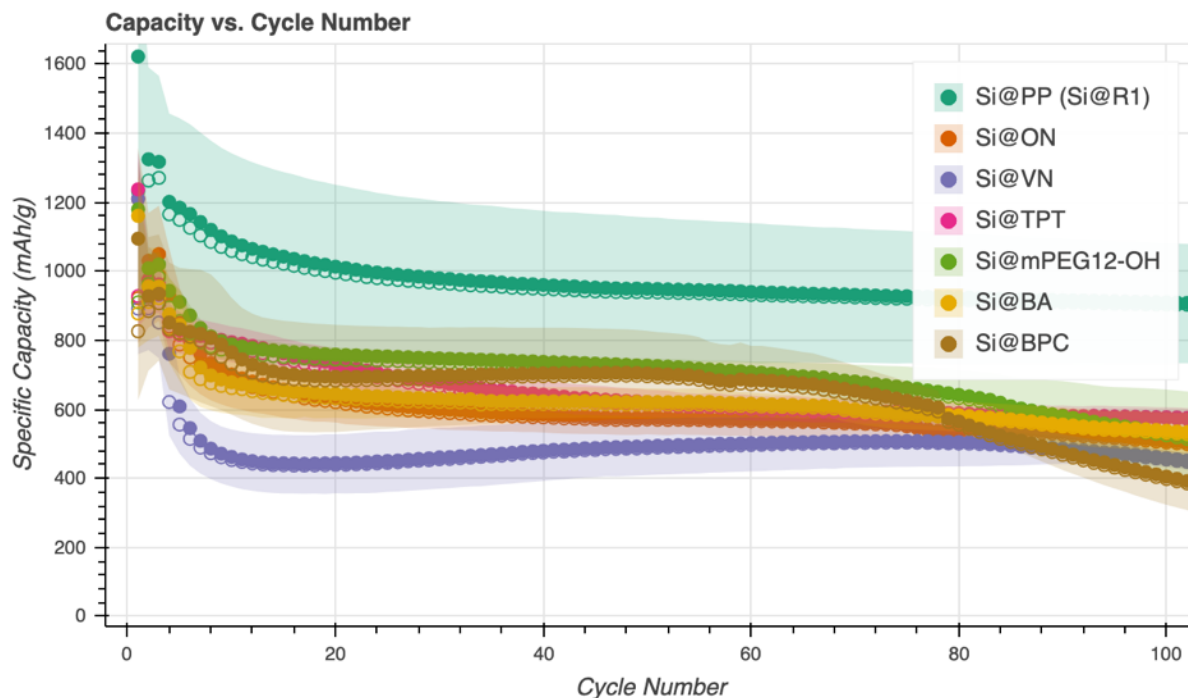
Figure S3. Specific capacity vs. cycle number of all the Si@R electrodes tested in this work and shown in Figure 3d in the main text. Solid circles are lithiation capacity, open circles are delithiation capacity of the Si@R electrodes, and colored shading is the standard deviation of the capacities calculated using data from triplicate cells. The legend labels correlate to the coating precursor molecules as follows: PP (4-phenyl phenol), ON (1-naphthol), VN (2-vinylnaphthalene), TPT (1,1',4',1"-terphenyl-4-thiol), mPEG12-OH (methoxy-PEG12-Hydroxyl), BA (benzaldehyde), BPC (biphenyl-4-carboxaldehyde). The capacities are normalized to all components in the electrode films (Si@R NPs, Timcal C65, and PAA binder). Each electrode exhibits a fairly stable specific capacity after the initial 20 cycles, though the specific capacity at which each stabilizes at is variable, suggesting different degrees of Si NP utilization depending on the coating. Rollover capacity decline can be observed for some of the electrodes starting between 60-80 cycles, which we attribute to electrolyte degradation and drying out. We discuss this rollover decline in more detail in a previous publication,[7] a phenomenon that is dependent on applied current density (changes depending on electrode areal loading) and that is exacerbated by the production of high surface area Li dendrites in the half-cells.

Full-cell assembly and electrochemical cycling

The Si@R$_1$ electrode was tested in triplicate in a full-cell with GenF electrolyte assembled with the following stack order: Negative cell case, coin cell gasket, 0.5 mm thick SS spacer, 15 mm diameter punch of Si@R1 electrode, 40 µL of electrolyte, 19 mm diameter punch of Celgard 2325, 14 mm punch of LFP cathode (Made by CAMP facility at Argonne National Lab, cathode ID LN3174-185-5: 90 wt% LFP, 5 wt% Timcal C45, 5% Solvay 5130 PVDF Binder, nominal 2.59 mAh/cm^2 loading), 0.5 mm thick SS spacer, wave spring, positive cell cap. The cell was sealed using a Hohsen automatic hydraulic crimper and allowed to rest for 4 h at open circuit potential before cycling using the following protocol: Cell was cycled 3 times at a C/20 rate (calculated using mass of electrode punch and specific capacity of Si NPs of 3500 mAh/g) between 2.7–3.45 V, followed by cycling with the same voltage cutoffs at a calculated rate of C/5.
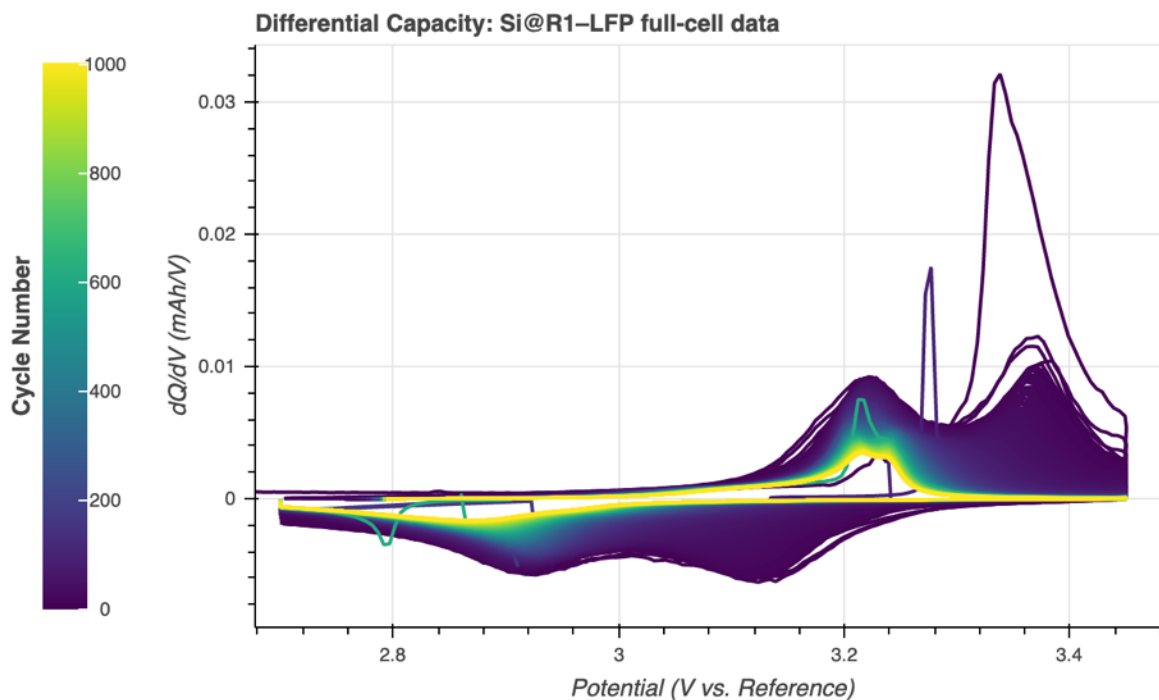
Figure S4. Differential capacity of a Si@R$_1$-LFP full-cell (Si NPs coated with 4-phenyl phenol) cycled for 1000 cycles. The corresponding capacity data for this cell is shown in Figures 3b and 3c in the main text. The Si@R$_1$ electrode behaves similarly to the half-cell shown in Figure S1 for the initial 4 cycles (the voltage scale is reversed in the full-cell compared to the half-cell). However, over the course of cycling, the (de)lithiation peaks diminish in intensity, with the higher voltage (de)lithiation peaks disappearing altogether. The fact that the lower voltage (de)lithiation peaks are still present is indicative that the capacity fade observed is indeed primarily due to Li-inventory consumption. By the end of cycling, there is just enough Li to only partially form the lower voltage Li$_x$Si phase before the LFP runs out of Li, polarizes to higher potentials, and the upper cutoff voltage is reached before the higher voltage Li$_x$Si phase can be formed. In contrast, if the capacity fade observed were due to active material loss or impedance growth, both the upper and lower (de)lithation peaks would diminish simultaneously or have their peak potentials shifted simultaneously, respectively.

Supplemental References

(1)   Mangolini, L.; Thimsen, E.; Kortshagen, U. High-Yield Plasma Synthesis of Luminescent Silicon Nanocrystals. *Nano Lett.* **2005**, *5*, 655–659. https://doi.org/10.1021/nl050066y.
(2)   Wheeler, L. M.; Anderson, N. C.; Palomaki, P. K. B.; Blackburn, J. L.; Johnson, J. C.; Neale, N. R. Silyl Radical Abstraction in the Functionalization of Plasma-Synthesized Silicon Nanocrystals. *Chem. Mater.* **2015**, *27*, 6869–6878. https://doi.org/10.1021/acs.chemmater.5b03309.
(3)   Carroll, G. M.; Schulze, M. C.; Martin, T. R.; Pach, G. F.; Coyle, J. E.; Teeter, G.; Neale, N. R. SiO2 Is Wasted Space in Single-Nanometer-Scale Silicon Nanoparticle-Based Composite Anodes for Li-Ion Electrochemical Energy Storage. *ACS Appl. Energy Mater.* **2020**, *3*, 10993–11001. https://doi.org/10.1021/acsaem.0c01934.
(4)   Smith, A. J.; Burns, J. C.; Trussler, S.; Dahn, J. R. Precision Measurements of the

Coulombic Efficiency of Lithium-Ion Batteries and of Electrode Materials for Lithium-Ion Batteries. *J. Electrochem. Soc.* **2010**, *157*, A196. https://doi.org/10.1149/1.3268129.

(5)   Harlow, J. E.; Ma, X.; Li, J.; Logan, E.; Liu, Y.; Zhang, N.; Ma, L.; Glazier, S. L.; Cormier, M. M. E. E.; Genovese, M.; Buteau, S.; Cameron, A.; Stark, J. E.; Dahn, J. R. A Wide Range of Testing Results on an Excellent Lithium-Ion Cell Chemistry to Be Used as Benchmarks for New Battery Technologies. *J. Electrochem. Soc.* **2019**, *166*, A3031–A3044. https://doi.org/10.1149/2.0981913jes.

(6)   Dahn, J. R.; Burns, J. C.; Stevens, D. A. Importance of Coulombic Efficiency Measurements in R & D Efforts to Obtain Long-Lived Li-Ion Batteries. *Electrochem. Soc. Interface* **2016**, *25*, 75–78. https://doi.org/10.1149/2.F07163if.

(7)   Schulze, M. C.; Carroll, G. M.; Martin, T. R.; Sanchez-Rivera, K.; Urias, F.; Neale, N. R. Hydrophobic versus Hydrophilic Interfacial Coatings on Silicon Nanoparticles Teach Us How to Design the Solid Electrolyte Interphase in Silicon-Based Li-Ion Battery Anodes. *ACS Appl. Energy Mater.* **2021**, *ASAP*. https://doi.org/10.1021/acsaem.0c02817.